Electronic Supplementary Material (ESI) for Catalysis Science & Technology.

Single-site, Ni-modified Wells–Dawson-type polyoxometalate for propylene dimerization

Galiya Magazova, Yoonrae Cho, Jessica A. Muhlenkamp and Jason C. Hicks*

Department of Chemical and Biomolecular Engineering, 250 Nieuwland Hall, University of Notre Dame, Notre Dame, IN 46556

1. Experimental Details

1.1 Characterization of Catalyst

1.1.1 Solution ^{31}P NMR of Ni-POM-WD and Wells-Dawson polyoxometalate derivatives

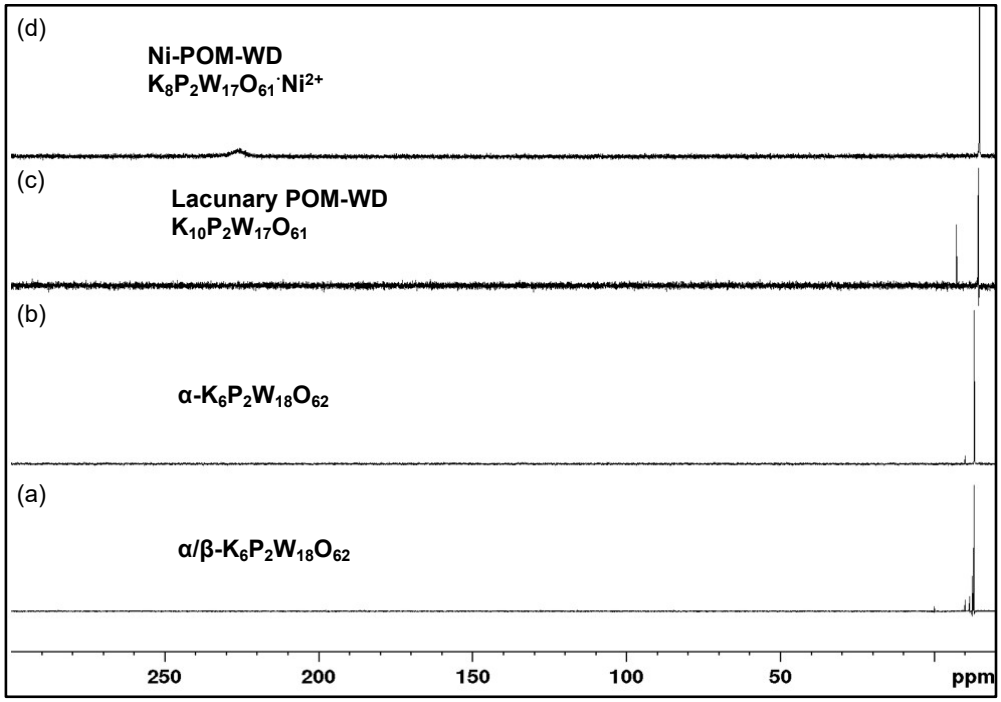

Figure S1. Solution ^{31}P NMR of a mixture α/β-$K_6P_2W_{18}O_{62}$ (a), α-$K_6P_2W_{18}O_{62}$ (b), lacunary POM-WD ($K_{10}P_2W_{17}O_{61}$) (c), and Ni-POM-WD ($K_8P_2W_{17}O_{61}{\cdot}Ni^{2+}$) (d)

1.1.2 N_2 Physisorption

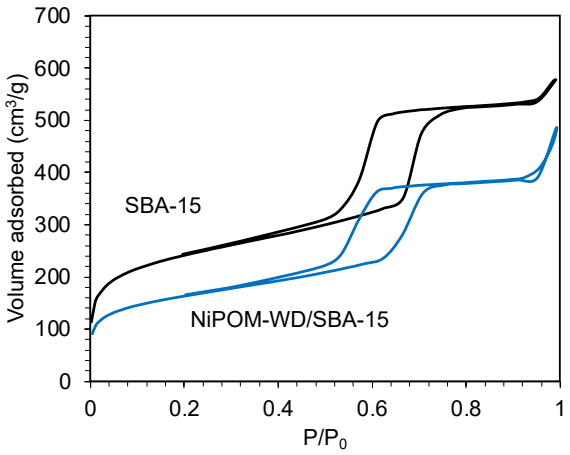

Figure S2. Nitrogen physisorption isotherms of SBA-15 and NiPOM-WD/SBA-15

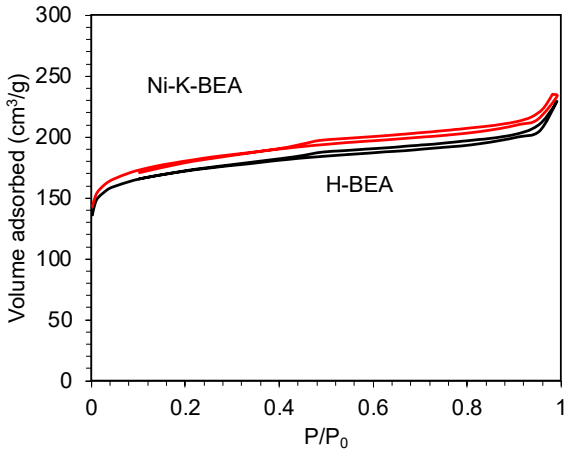

Figure S3. Nitrogen physisorption isotherms of H-BEA and Ni-K-BEA

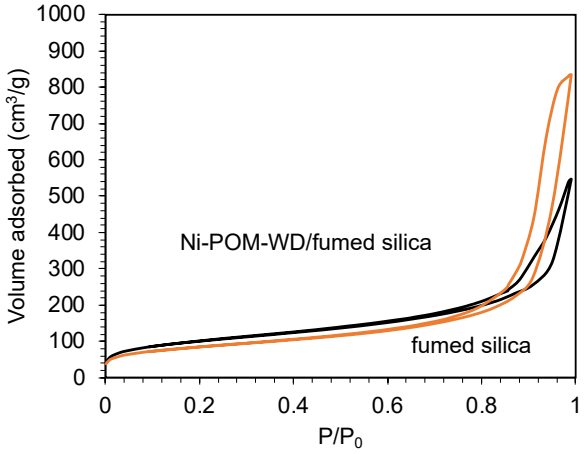

Figure S4. Nitrogen physisorption isotherms of fumed silica and Ni-POM-WD/fumed silica

Table S1. Elemental analysis and nitrogen physisorption pore properties of Ni-POM-WD/SBA-15 (1wt% Ni-POM-WD), fumed silica, Ni-POM-WD/fumed silica (10wt% Ni-POM-WD)

Sample	Elemental analysis (Ni wt%)	BET Surface Area (m^2/g)	BJH Adsorption Pore Diameter (Å)	Total Pore Volume (cm^3/g)
Fumed silica	-	354	-	0.69
Ni-POM-WD/fumed silica	0.12	297	-	1.21

1.1.3 Solid-state MAS ^{31}P NMR of Ni-POM-WD/SBA-15.

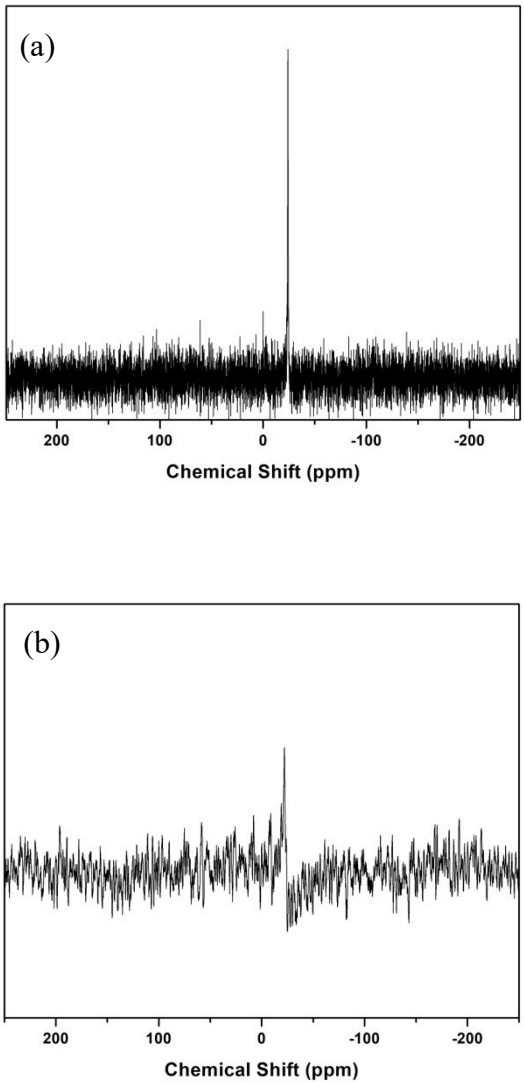

Figure S5. Solid state MAS ^{31}P NMR of fresh Ni-POM-WD/SBA-15 (a) and spent Ni-POM-WD/SBA-15 (b) after propylene oligomerization reaction at 180°C and 1 bar

1.1.4 High-angle annular dark-field scanning transmission electron microscopy (HAADF STEM) and energy dispersive X-ray spectroscopy (EDX) mapping

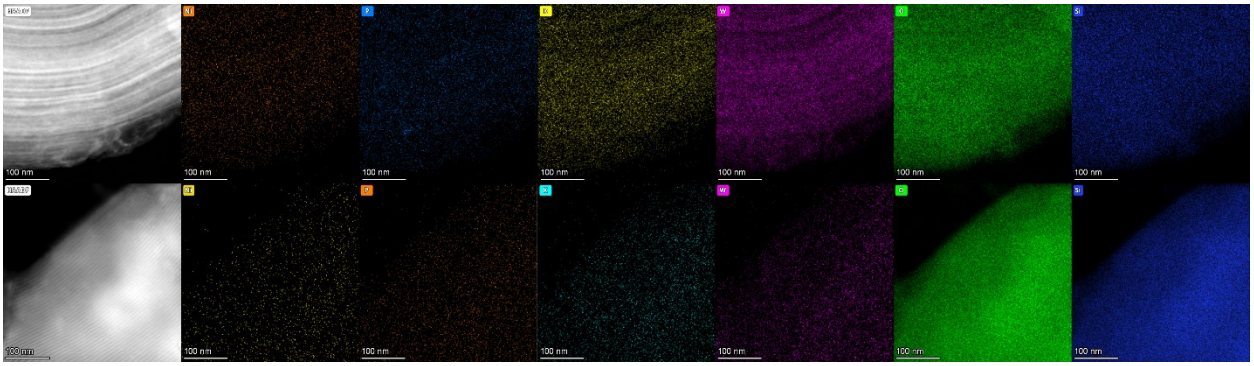

Figure S6. HAADF-STEM image and EDX elemental mapping (Ni, P, K, W, O, Si) of fresh Ni-POM-WD/SBA-15 (top) and spent Ni-POM-WD/SBA-15 (bottom) after propylene oligomerization reaction at 180°C and 1 bar

1.2 Thermogravimetric analysis (TGA)

The thermogravimetric analysis (TGA) of the fresh and spent Ni-POM-WD/SBA-15 was performed on a Mettler Toledo Star 1 machine. The sample was heated from 25°C to 800°C with 5°C /min ramp rate using dry air flow at 20 ml/min.

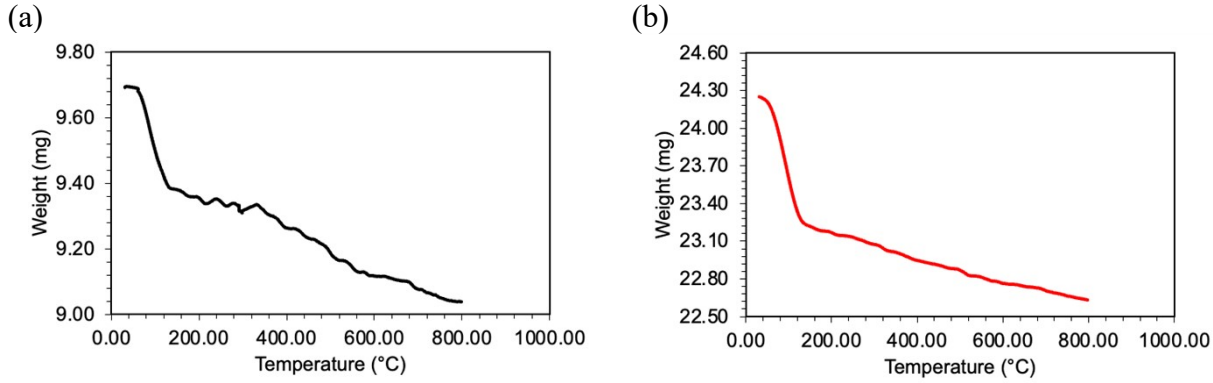

Figure S7. Thermogravimetric profile of fresh catalyst (a), spent catalyst after reaction-regeneration cycles (b)

2. Additional propylene oligomerization results

2.1 Product distribution at steady-state conversion for Ni-POM-WD/SBA-15 and Ni-K-BEA

The steady-state conversion and selectivity were measured by averaging the values after 300 min time on stream.

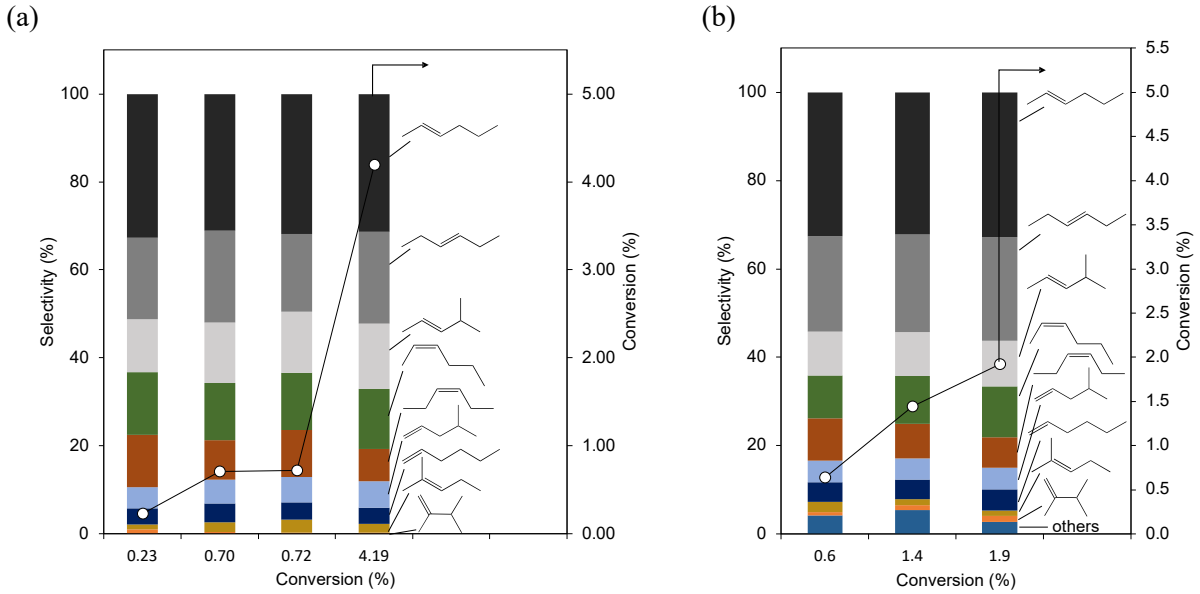

Figure S8. Propylene oligomerization product selectivity at steady-state conversions at 180°C for Ni-POM-WD/SBA-15 (a) and Ni-K-BEA (b).

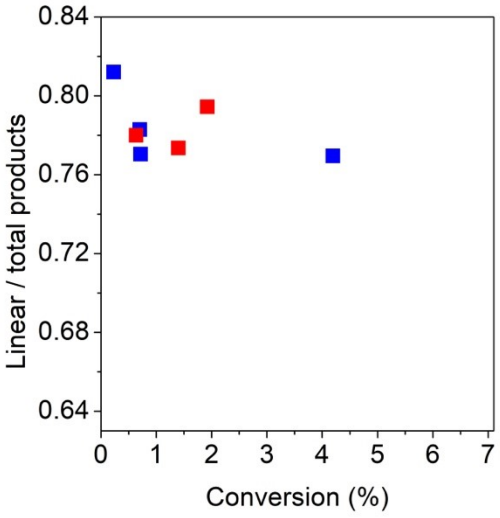

Figure S9. Selectivity for linear products at steady-state conversions at 180°C for Ni-POM-WD/SBA-15 (blue) and Ni-K-BEA (red).

2.2 Product distribution for Ni-POM-WD/SBA-15 and Ni-POM-WD/fumed silica at initial conversions

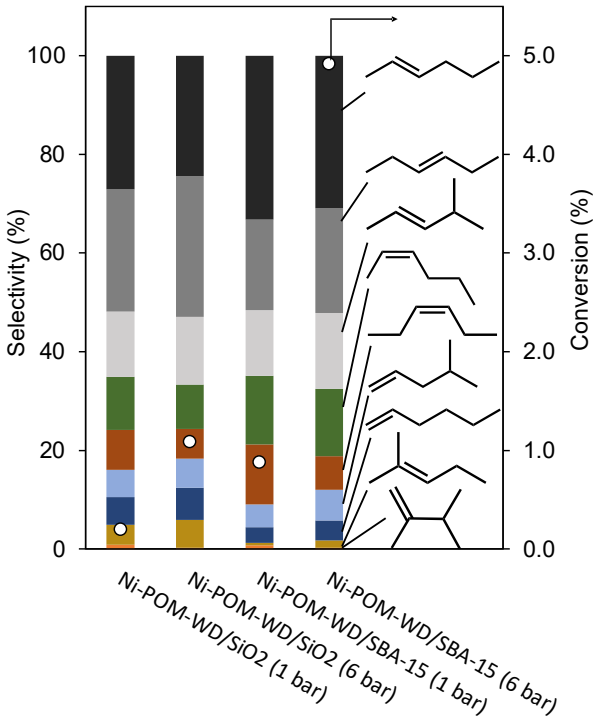

(a)

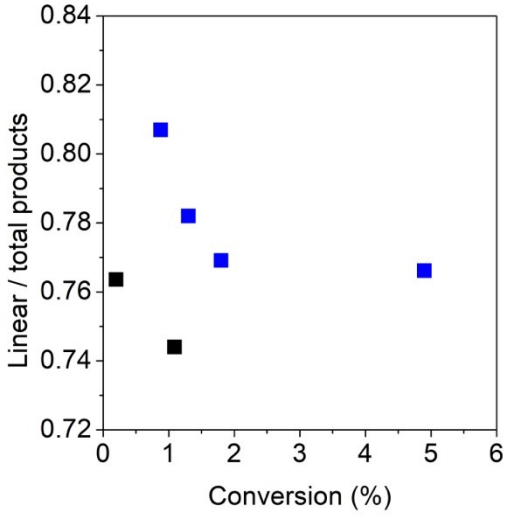

(b)

Figure S10. Propylene oligomerization product selectivity at initial conversions at 180°C for Ni-POM-WD/fumed silica and Ni-POM-WD/SBA-15 (a) and selectivity for linear products on Ni-POM-WD/fumed silica (black) and Ni-POM-WD/SBA-15 (blue) (b)

2.2 Space velocity sweep experiments for Ni-POM-WD/SBA-15

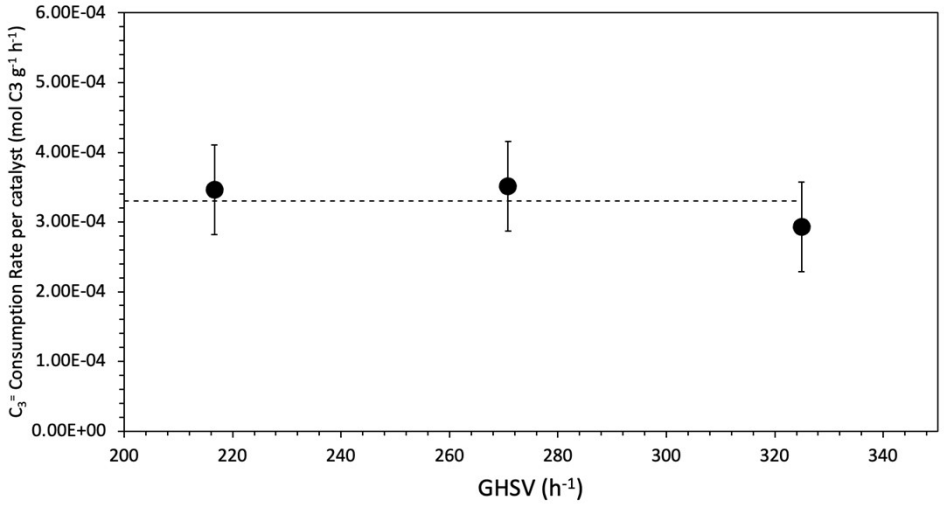

Figure S11. Propylene consumption rate normalized per weight for Ni-POM-WD/SBA-15 at 180°C, 1.01 pressure, ~0.33 propylene mole fraction, 8, 10, 12 mL/min total flowrate.

3. Propylene oligomerization model

Table S2. Kinetic expressions for propylene oligomerization

Reaction step	Chemical Equations [a]	Kinetic expressions [b]
Adsorption	$C_3H_6 + * \rightleftarrows *- C_3H_6$	$K_A = \frac{\theta_{*-C_3H_6}}{P_{C_3H_6}\theta_*}$
Coupling	$*- C_3H_6 + C_3H_6 \rightleftarrows *- C_6H_{12}$	$r_c = k_c P_{C_3H_6} \theta_{*-C_3H_6}$
Desorption	$*- C_6H_{12} \rightleftarrows C_6H_{12} + *$	$K_D = \frac{P_{C_6H_{12}}\theta_*}{\theta_{*-C_6H_{12}}}$
Balance of active sites	$1 = \theta_* + \theta_{*-C_3H_6} + \theta_{*-C_6H_{12}}$ $1 = \theta_* + K_A P_{C_3H_6}\theta_* + \frac{P_{C_6H_{12}}\theta_*}{K_D} = \left(1 + K_A P_{C_3H_6} + \frac{P_{C_6H_{12}}}{K_D}\right)\theta_*$ $\theta_* = \frac{1}{1 + K_A P_{C_3H_6} + \frac{P_{C_6H_{12}}}{K_D}}$ $\theta_{*-C_3H_6} = \frac{K_A P_{C_3H_6}}{1 + K_A P_{C_3H_6} + \frac{P_{C_6H_{12}}}{K_D}}$	
Coupling		$r_c = \frac{k_c K_A P_{C_3H_6}^2}{1 + K_A P_{C_3H_6} + \frac{P_{C_6H_{12}}}{K_D}}$
$P_{C_6H_{12}} \ll 1$ [c]		$r_c = \frac{k_c K_A P_{C_3H_6}^2}{1 + K_A P_{C_3H_6}}$
$K_A P_{C_3H_6} \ll 1$ [d]		$r_c = k_c K_A P_{C_3H_6}^2$
$K_A P_{C_3H_6} \gg 1$ [e]		$r_c = k_c P_{C_3H_6}$

[a] The active site is represented by *

[b] K_i represents equilibrium constant, P_i is the partial pressure of species i, k_i reaction constant, θ_* fraction of active sites

[c] At low propylene conversion assuming low partial pressure of hexenes

[d] Second reaction rate order at low propylene partial pressure

[e] First reaction rate order at low propylene partial pressure

4. Stability of Ni-POM-WD

4.1 First-order deactivation model[1,2]:

$$r\,(t) = r_i e^{-k_d t} + r_{ss} \#(S1)$$

where r is the rate at a given time, r_i initial rate value for the time-dependent component, k_d is the deactivation constant, r_{ss} is the steady-state rate. Rate at t=0 is calculated as $r_0=r_i+r_{ss}$. The steady-state rate parameter is added because the deactivated catalyst value in the given TOS range does not reach zero.

4.2 Second-order deactivation model[1,2]:

$$r = \frac{r_i}{1 + k_d t} + r_{ss} \#(S2)$$

where r is the rate at a given time, r_i initial rate value for the time-dependent component, k_d is the deactivation constant, r_{ss} is the steady-state rate. Rate at t=0 is calculated as $r_0=r_i+r_{ss}$. The steady-state rate parameter is added because the deactivated catalyst value in the given TOS range does not reach zero.

4.3 Butt-Peterson deactivation model[1,2]:

$$r = \frac{r_i}{\left[1 + (n-1) k_d {r_o}^{(n-1)} t\right]^{\left(\frac{1}{n-1}\right)}} + r_{ss} \#(S3)$$

where r is the rate at a given time, r_i initial rate value for the time-dependent component, k_d is the deactivation constant, r_{ss} is the steady-state rate, n is the deactivation order. Rate at t=0 is calculated as $r_0=r_i+r_{ss}$. The steady-state rate parameter is added because the deactivated catalyst value in the given TOS range does not reach zero.

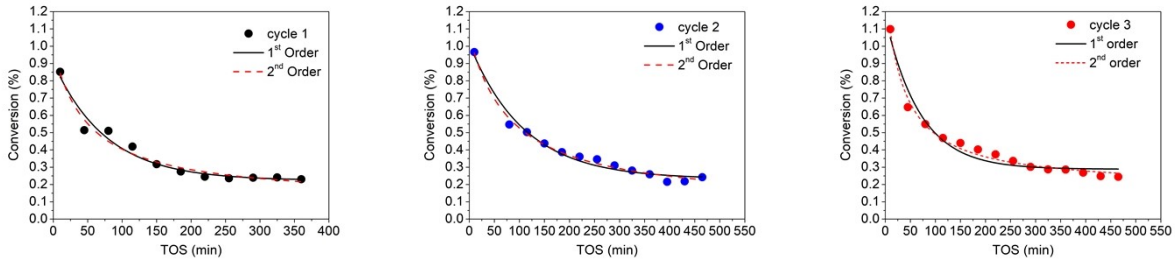

Figure S12. Fit of propylene conversion data to 1st and 2nd order deactivation profiles on Ni-POM-WD/SBA-15 (10wt% Ni-POM-WD) at 180°C and 1 bar during 3 reaction-regeneration cycles

(a) (b)

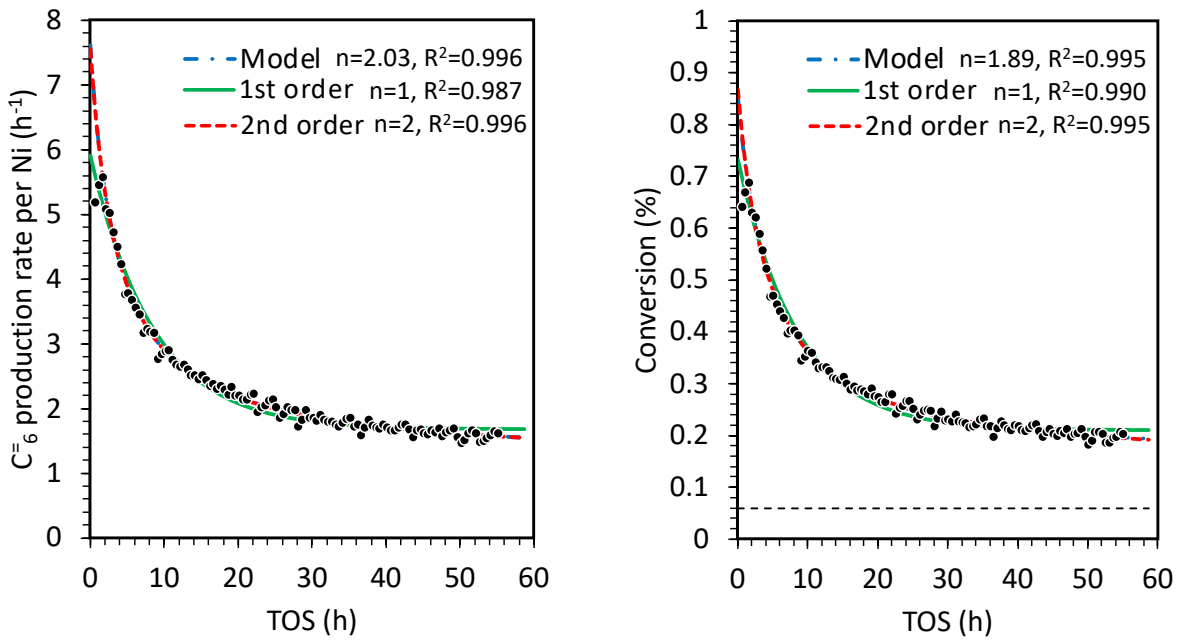

Figure S13. Fit of propylene consumption rate (a) and conversion data (b) to 1st, 2nd order deactivation profiles and Butt-Peterson deactivation model on Ni-POM-WD/SBA-15 (10wt% Ni-POM-WD or 0.12wt% Ni) at 180°C and 1 bar. The background thermal conversion is noted by the dash line (---).

Table S3. Deactivation model parameters for propylene oligomerization rates on Ni-POM-WD/SBA-15 (10wt% Ni-POM-WD) at 180°C and 1 bar fitted to 1st, 2nd, and Butt-Peterson deactivation models.

Model	r_0 (mol $C^{=}_6$ /mol Ni/h)	r_{ss} (mol $C^{=}_6$ /mol Ni/h)	k_d (h^{-1})	n	R^2	Normalized absolute error (%) [a]
1st order	5.91	1.68	0.118	1	0.987	4.34
2nd order	7.55	1.17	0.268	2	0.996	2.66
Butt-Peterson	7.61	1.15	0.040	2.03	0.996	2.66

[a] $Normalized\ absolute\ error = \sum \frac{\sqrt{(predicted\ rates\ -\ experimental\ rates)^2}}{experimental\ rates} \times 100\%$

(a) (b)

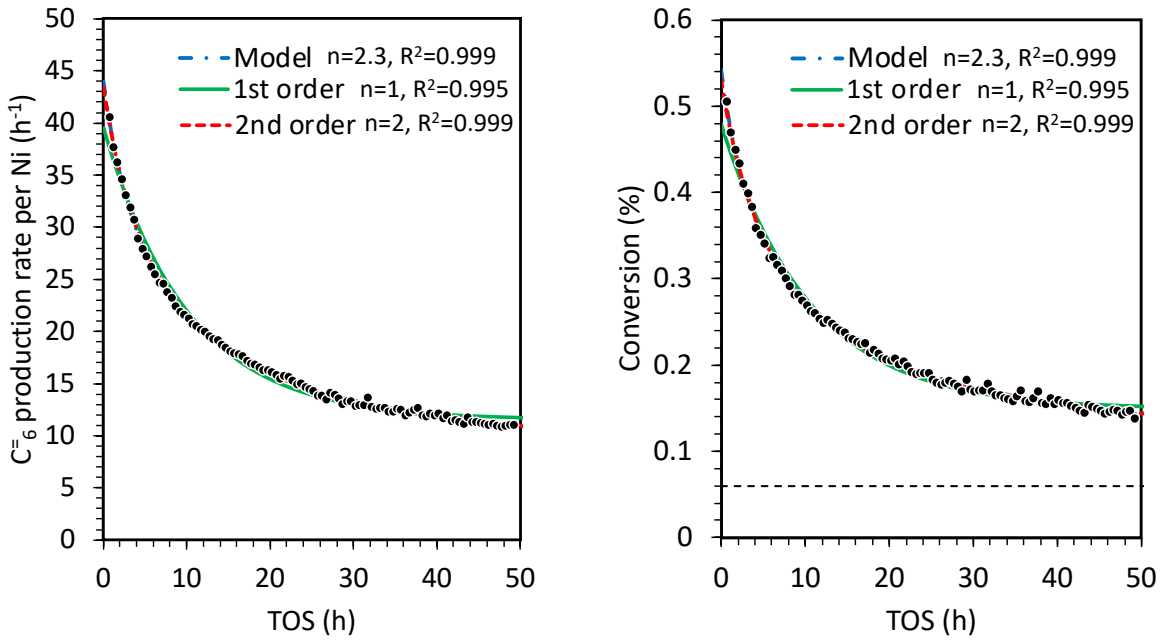

Figure S14. Fit of propylene consumption rate (a) and conversion data (b) to 1st, 2nd order deactivation profiles and Butt-Peterson deactivation model on Ni-POM-WD/SBA-15 (1wt% Ni-POM-WD or 0.011wt% Ni) at 180°C and 1 bar. The background thermal conversion is noted by the dash line (---).

Table S4. Deactivation model parameters for propylene oligomerization rates on Ni-POM-WD/SBA-15 (10wt% Ni-POM-WD) at 180°C and 1 bar fitted to 1st, 2nd, and Butt-Peterson deactivation models.

Model	r_0 (mol $C^{=}_6$ /mol Ni/h)	r_{ss} (mol $C^{=}_6$ /mol Ni/h)	k_d (h^{-1})	n	R^2	Normalized absolute error (%) [a]
1st order	39.55	11.51	0.099	1	0.995	3.15
2nd order	43.35	6.46	0.146	2	0.999	1.39
Butt-Peterson	43.90	4.55	0.0013	2.3	0.999	1.29

[a] $Normalized\ absolute\ error = \sum \frac{\sqrt{(predicted\ rates\ -\ experimental\ rates)^2}}{experimental\ rates} \times 100\%$

(a) (b)

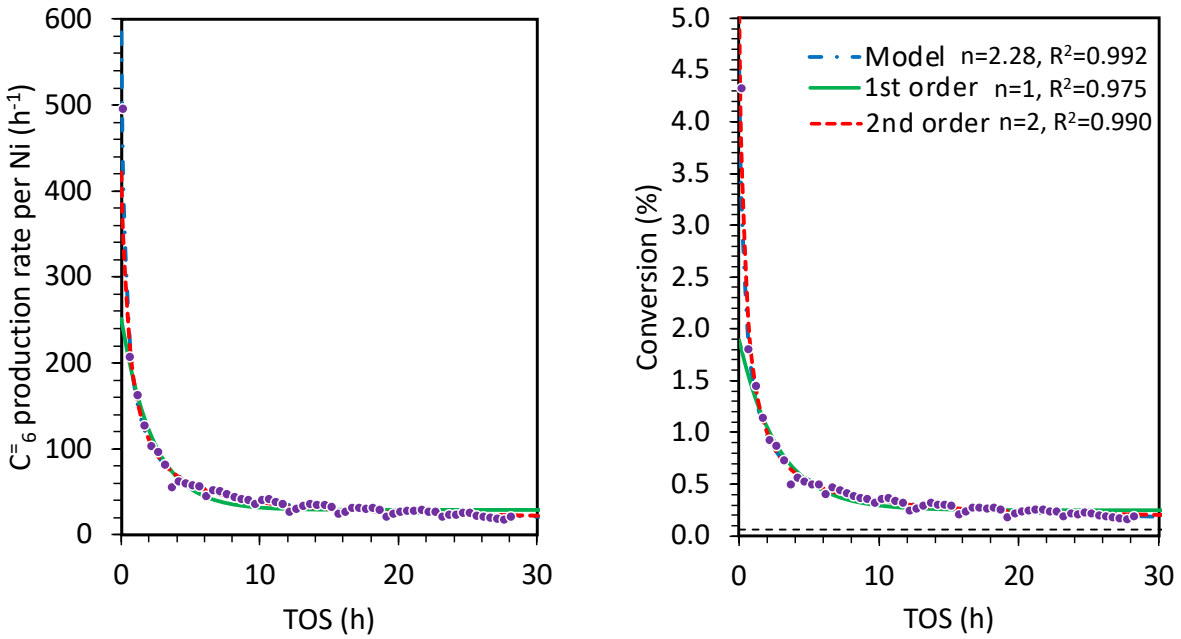

Figure S15. Fit of propylene consumption rate (a) and conversion data (b) to 1st, 2nd order deactivation profiles and Butt-Peterson deactivation model on Ni-K-BEA at 180°C and 1 bar. The background thermal conversion is noted by the dash line (---).

Table S5. Deactivation model parameters for propylene oligomerization rates on Ni-K-BEA at 180°C and 1 bar fitted to 1st, 2nd, and Butt-Peterson deactivation models.

Model	r_0 (mol $C^{=}_{6}$ /mol Ni/h)	r_{ss} (mol $C^{=}_{6}$ /mol Ni/h)	k_d (h^{-1})	n	R^2	Normalized absolute error (%) [a]
1st order	251.1	29.03	0.439	1	0.981	16.4
2nd order	420.9	13.99	1.607	2	0.993	8.96
Butt-Peterson	584.6	7.24	0.0008	2.3	0.993	8.52

[a] $Normalized\ absolute\ error = \sum \frac{\sqrt{(predicted\ rates\ -\ experimental\ rates)^2}}{experimental\ rates} \times 100\%$

5. Heat and mass transfer calculation for propylene dimerization on Ni-POM-WD/SBA-15

5.1 The Weisz–Prater criterion for internal diffusion[3]

Internal mass transfer limitations can be neglected if

$$C_{WP} = \frac{-r_{C3}\rho_c R^2}{D_e C_{C3}} < 1$$

where, $^{-r_{C3}}$ is observed reaction rate [g propylene/kg cat • h], $^{\rho_c}$ is solid catalyst density [kg/m^3], ^{R} is catalyst particle radius [m], ^{D_e} is effective diffusivity [m^2/h], $^{C_{C3}}$ is concentration of propylene on catalyst surface [g propylene/m^3].

Effective diffusivity of propylene-hexene mixture was calculated by Wilker's equation,[4]

$D_e = \frac{1}{\frac{y'_{C6}}{D_{C3-C6}}} = \frac{D_{C3-C6}}{\frac{y_{C6}}{(1-y_{C6})}}$. Where, $^{D_{C3-C6}}$ was calculated using the Chapman-Enskog equation,[4]

$D_{C3-C6} = \frac{0.001858T^{3/2}\sqrt{\frac{M_{C3}+M_{C6}}{M_{C3}M_{C6}}}}{p\sigma_{12}^2\Omega_{D,12}}$, where M is the molecular weight [g/mol], T is temperature [K], p total pressure [atm], $^{\sigma_{12}}$is Lennard-Jones force constant, $^{\Omega_{D,12}}$ is collision integral function.

The Weisz–Prater criterion was used to assess the internal diffusion limitations,

$$C_{WP} = \frac{-r_{C3}\rho_c R^2}{D_e C_{C3}} < 1$$

resulted in 3.5×10^{-10}–2.2×10^{-9}<1, which implies no internal diffusion limitations.

5.2 The Mears criterion for external diffusion[5]

External mass transfer effects can be neglected if

$$\frac{-r_{C3}\rho_b Rn}{k_c C_{C3}} < 0.15$$

where, $^{r_{C3}}$ is observed reaction rate [kmol/kg cat •s], $^{\rho_b}$ is bulk density of catalyst bed [kg/m^3], R is catalyst particle radius [m], n is reaction order, ^{k_c} is ass transfer coefficient [m/s], $^{C_{C3}}$ is bulk gas concentration [kmol/m^3].

The Mears criterion for external diffusion,

$$\frac{-r_{C3}\rho_b Rn}{k_c C_{C3}} < 0.15$$

gave 7.2×10^{-5}–1.9×10^{-3}<0.15, which indicates no external mass transfer effects.

5.3 The Mears criterion for heat transport limitation[5]

Heat transport limitations are negligible if

$$\frac{-\Delta Hr_{C3}R_p}{hT_b} < 0.15\frac{RT_b}{A_E}$$

where, ΔH is heat of reaction [kJ/mol], r_{C3} is reaction rate per unit volume [mol/m^3], R_p is particle diameter [m], h is heat transfer coefficient [kJ/m^2 K s], T_b is temperature of bulk fluid [K], R is ideal gas constant [kJ/mol K], A_E is activation energy [kJ/mol].

The Mears criterion for heat transport limitation,

$$\frac{-\Delta H r_{C3} R_p}{h T_b} < 0.15 \frac{R T_b}{A_E}$$

resulted in 1.5×10^{-5}–2.3×10^{-4}<0.15, which implies absence of heat transport limitations.

References

1 A. Saxena, R. Joshi, R. R. Seemakurthi, E. Koninckx, L. J. Broadbelt, J. Greeley and R. Gounder, *ACS Engineering Au*, 2022, **2**, 12–16.

2 R. Caulkins, R. Joshi, R. Gounder and F. H. Ribeiro, *ChemCatChem*, , DOI:10.1002/cctc.202101478.

3 P. B. Weisz and C. D. Prater, in *Advances in Catalysis*, eds. W. G. Frankenburg, V. I. Komarewsky and E. K. Rideal, Academic Press, 1954, vol. 6, pp. 143–196.

4 R. B. Bird, W. E. Stewart and E. N. Lightfoot, *Transport Phenomena, Revised 2nd Edition*, John Wiley & Sons, 2006.

5 D. E. Mears, *Industrial & Engineering Chemistry Process Design and Development*, 1971, **10**, 541–547.